Mode-coupling theory and molecular dynamics simulation for heat conduction in a chain with transverse motions

Jian-Sheng Wang

Singapore-MIT Alliance and Department of Computational Science,
National University of Singapore, Singapore 117543, Republic of Singapore

Baowen Li

Department of Physics, National University of Singapore, Singapore 117542, Republic of Singapore

We study heat conduction in a one-dimensional chain of particles with longitudinal as well as transverse motions. The particles are connected by two-dimensional harmonic springs together with bending angle interactions. The problem is analyzed by mode-coupling theory and compared with molecular dynamics. We find very good, quantitative agreement for the damping of modes between a full mode-coupling theory and molecular dynamics result, and a simplified mode-coupling theory gives qualitative description of the damping. The theories predict generically that thermal conductance diverges as $N^{1/3}$ as the size N increases for systems terminated with heat baths at the ends. The $N^{2/5}$ dependence is also observed in molecular dynamics which we attribute to crossover effect.

PACS numbers: 44.10.+i, 05.45.–a, 05.70.Ln, 66.70.+f

I. INTRODUCTION

The problem of heat conduction is a well-studied field. More than two centuries ago, Joseph Fourier summarized the behavior of heat conduction by the law that bears his name. This law describes phenomenologically that the heat current is proportional to the temperature gradient. The detailed atomistic theories of heat conduction appeared only much later. For heat conduction in gas, the simple kinetic theory gives the result $\kappa = \frac{1}{3}C\bar{v}\bar{l}$, where C is specific heat, $\bar{v}$ is average velocity and $\bar{l}$ is mean-free path. Peierls' theory of heat conduction in insulating solids [1] is a classic on this subject. These early theories deal with mostly the relevant three dimensions. It turns out that low dimensional systems are more interesting and in some sense strange. An analysis of a simple one-dimensional (1D) harmonic oscillator model shows [2] that there is no well-defined temperature gradient, the thermal conductivity diverges with system sizes as $N^{1/2}$ or N, depending on the boundary conditions. There is a general argument, for momentum conserving systems, that the thermal conduction in 1D is necessarily divergent [3].

There have been many analytical and numerical studies of 1D heat conduction (see ref. [4] and [5] for review). We'll mention some of the most relevant papers to current work. The work of Lepri *et al* [6] by mode-coupling theory and molecular dynamics suggests a divergent thermal conductivity exponent of 2/5, i.e., $\kappa \propto N^{2/5}$ for a 1D chain model with Fermi-Pasta-Ulam (FPU) interactions. Mode-coupling theory is usually applied in the dynamics of liquids [7, 8]. The first use of this theory in the context of heat conduction appears only recently, mostly due to Lepri and his collaborators [9]. Perverzev analyzed the same problem with the Peierls theory for phonon gas and gave the same conclusion of 2/5 exponent [10]. The

result of 2/5 is also supported by numerical simulation from several groups [11, 12, 13, 14]. These results are supposed to be universal to some extent. However, it is challenged by a different result of 1/3 by Narayan and Ramaswamy [15], based on fluctuating hydrodynamics and renormalization group analysis. The numerical result for this 1/3 law is not convincing, as for the same model – the hard-particle gas model – some obtained 1/3 [16, 17], while others obtained different value 1/4 [18]. But for the FPU model, there is no good evidence for an exponent of 1/3 [19].

When momentum conservation is broken such as the one with on-site potential, the heat conduction can become normal again like the Frenkel-Kontorova model [20] and the ϕ^4 model [14, 21].

In order to understand the underlying microscopic dynamical mechanism of the Fourier law, a different class of models – billiard channels – have been introduced and studied in recent years [22, 23]. Various exponent values are found in such systems. Thus, it is believed that a universal constant does not exist at all. Instead, the divergent (convergent) exponent of the thermal conductivity is found related to the power of super (sub) diffusion [23].

Besides the theoretical significance of heat conduction research in low dimensional systems, it is also of practical importance. Recent development of nanotechnology will enable us to manufacture devices with feature sizes at molecular level. The understanding of heat conduction mechanism will allow us to control and manipulate heat current, and eventually to design novel thermal devices with certain function [24]. To this end, more realistic physical models are necessary. Among many others, nanotubes and polymer chains are most promising. There have been a number of numerical works to compute the thermal conductivity of the Carbon nanotubes [25, 26].

Recent molecular dynamics (MD) study of Carbon nanotubes with realistic interaction potential suggested a divergent thermal conductivity for narrow diameter tubes [27, 28]. The quantum effect of such systems is also very interesting [29, 30].

We study the heat conduction of a 1D solid, as a classical system. A brief version of this paper is reported in ref. [31]. In the rest of the paper, we introduce the quasi-one-dimensional chain model in Sec. II. We discuss the basis of the mode-coupling theory, the projection method in Sec. III. The mode-coupling approximations and their numerical and analytical solutions are discussed in Sec. IV and V. The basic output of the mode-coupling analysis is the dependence of damping of the modes with the wave-vector of the modes. We find that the transverse modes are diffusive, with $\gamma_p^\perp \propto p^2$, while the longitudinal modes are super-diffusive, $\gamma_p^\parallel \propto p^{3/2}$, where γ_p is the decay rate for mode with momentum or lattice wave number p. We discuss the relationship between the damping of the modes with the heat conductivity through Green-Kubo formula in Sec. VI. Our mode-coupling theory predicts that the heat conductance diverges with the $1/3$ exponent when the transverse motions are important, while $2/5$ is recovered if the transverse motions can be neglected. In Sec. VII, we present nonequilibrium molecular dynamics results (with heat baths) of heat conductance and compare with mode-coupling theory. We conclude in the last section.

II.   CHAIN MODEL

Most of the previous studies considered only strictly 1D models, with the Fermi-Pasta-Ulam (FPU) model as the most representative. The strictly 1D models may not be applicable to real systems such as the nanotubes. Real systems of nanotubes or wires live in three-dimensional space. The added transverse motion and the flexibility of the tube at long length scales will certainly scatter phonons, and thus should have a profound effect on thermal transport.

While a direct simulation of a realistic system such as a polyethelene chain with empirical force fields such as that in refs. [32, 33] or nanotube with Tersoff potential [34] is possible, we think it is useful to consider a simplified model which captures one of the important features of the real systems – transverse degrees of freedom. Therefore we propose to study the following chain model in two dimensions [31]:

$$H(\mathbf{p}, \mathbf{r}) = \sum_i \frac{\mathbf{p}_i^2}{2m} + \frac{1}{2} K_r \sum_i \Big(|\mathbf{r}_{i+1} - \mathbf{r}_i| - a \Big)^2$$
$$+ K_\phi \sum_i \cos \phi_i, \tag{1}$$

where the position vector $\mathbf{r} = (x, y)$ and momentum vector $\mathbf{p} = (p_x, p_y)$ are two-dimensional; a is lattice constant. The minimum energy state is at $(ia, 0)$ for $i = 0$

to $N - 1$. If the system is restricted to $y_i = 0$ (corresponding to $K_\phi = +\infty$), it is essentially a 1D gas with harmonic interaction. The coupling K_r is the spring constant; K_ϕ signifies bending or flexibility of the chain, while ϕ_i is the bond angle formed with two neighboring sites, $\cos \phi_i = -\mathbf{n}_{i-1} \cdot \mathbf{n}_i$, and unit vector $\mathbf{n}_i = \Delta \mathbf{r}_i / |\Delta \mathbf{r}_i|$, $\Delta \mathbf{r}_i = \mathbf{r}_{i+1} - \mathbf{r}_i$.

Unlike the FPU model which does not have an energy scale, the second bond-angle bending term introduces an energy scale. In this work, we take mass $m = 1$, spring constant $K_r = 1$, and the Boltzmann constant $k_B = 1$, thus the most important parameters are K_ϕ and temperature T.

III.   PROJECTION METHOD

A.   Basic theory of projection

We follow the formulation of the projection method in ref. [35]. Let

$$A = \begin{pmatrix} a_1 \\ a_2 \\ \vdots \\ a_n \end{pmatrix} \tag{2}$$

be a column vector of n components of some arbitrary functions of dynamical variables (p, q). Each of the function $a_j(p, q)$ can be complex. Later, we shall choose a_j to be the canonical coordinates of the system. We use $A^\dagger = (a_1^*, a_2^*, \cdots, a_n^*)$ to denote the Hermitian conjugate of A. The equation of motion for A is

$$\dot{A}_t = \mathcal{L} A_t, \quad \text{or} \quad \dot{a}_j(t) = \mathcal{L} a_j(t), \tag{3}$$

where $\mathcal{L}$ is the Liouville operator

$$\mathcal{L} = -\sum \frac{\partial H}{\partial q} \frac{\partial}{\partial p} + \sum \frac{\partial H}{\partial p} \frac{\partial}{\partial q}. \tag{4}$$

Equation (3) can be viewed as a partial differential equation with variables (p, q) and time t. $A_t \equiv A(p_t, q_t) = A(t, p, q)$, i.e., the quantity A at time t when the initial condition at $t = 0$ is (p, q). Quantity without a subscript t will be understood to be evaluated at time $t = 0$, e.g., $p = p_{t=0} = p(0)$. A formal solution to Eq. (3) is simply $A_t = e^{t\mathcal{L}} A(p, q)$.

The projection operator on a column vector X is defined by

$$\mathcal{P} X = \langle X, A^\dagger \rangle \langle A, A^\dagger \rangle^{-1} A, \tag{5}$$

where $\langle X, A^\dagger \rangle$ and $\langle A, A^\dagger \rangle$ are $n \times n$ matrices. The angular brackets denote thermodynamical average in a canonical ensemble at temperature T. The comma separating the two terms is immaterial, but we use a notation of inner product. One can verify that $\mathcal{P}$ is indeed a projection operator, i.e., $\mathcal{P}^2 = \mathcal{P}$.

If we apply the projection operator $\mathcal{P}$ and $\mathcal{P}' = 1 - \mathcal{P}$ to the equation of motion, we get two coupled equations. Solving formally the second equation associated with $\mathcal{P}'$, and substituting it back into the first equation, we obtain an equation for the projected variable that formally resembles a Langevin equation:

$$\dot{A}_t = i\Omega A_t - \int_0^t \Gamma(t - s)A_s \, ds + R_t, \qquad (6)$$

where $i = \sqrt{-1}$ is the complex unit, and

$$\Gamma(t) = \langle R_t, R_0^\dagger \rangle \langle A, A^\dagger \rangle^{-1}, \qquad (7)$$

$$i\Omega = \langle \dot{A}, A^\dagger \rangle \langle A, A^\dagger \rangle^{-1}, \qquad (8)$$

$$R_t = e^{t\mathcal{P}'\mathcal{L}} R_0, \quad R_0 = \dot{A} - i\Omega A = \mathcal{P}'\mathcal{L}A. \qquad (9)$$

This set of equations is deterministic and formally exact. The only assumption made is that equilibrium distribution can be realized.

What is more important is the correlation functions, which are physical observables. We define the normalized correlation function (correlation matrix) as

$$G(t) = \langle A_t, A_0^\dagger \rangle \langle A, A^\dagger \rangle^{-1}. \qquad (10)$$

It is an identity matrix at $t = 0$ and has the property that $\dot{G}(0) = i\Omega$. From Eq. (6) we have,

$$\dot{G}(t) = i\Omega G(t) - \int_0^t \Gamma(t - s)G(s) \, ds. \qquad (11)$$

This equation can be solved formally using proper initial condition with a Fourier-Laplace transform,

$$G[z] = \int_0^\infty e^{-izt} G(t) \, dt, \qquad (12)$$

and similarly for $\Gamma(t)$. The solution is

$$G[z] = \left(i(z - \Omega) + \Gamma[z]\right)^{-1}. \qquad (13)$$

To simplify notation, we have used parentheses (e.g., $G(t)$) for functions in time domain, and square brackets with the same symbol (e.g., $G[z]$) for their corresponding Fourier-Laplace transform in frequency domain.

The information about the system is in the memory kernel $\Gamma(t)$. However, such a correlation function is difficult to calculate, since the evolution of the "random force" R_t does not follow the dynamics of the original Hamiltonian system. For example, it is impossible to compute directly R_t from molecular dynamics. For this reason, a "true force" can be introduced which obeys the normal evolution, i.e.,

$$F_t = e^{t\mathcal{L}} R_0 = \dot{A}_t - i\Omega A_t. \qquad (14)$$

The correlation function of the true force,

$$\Gamma_F(t) = \langle F_t, F_0^\dagger \rangle \langle A, A^\dagger \rangle^{-1}, \qquad (15)$$

and that of the random force are related in Fourier space as [35]

$$\Gamma[z]^{-1} = \Gamma_F[z]^{-1} - \left(i(z - \Omega)\right)^{-1}. \qquad (16)$$

This completes the formal theory of projection due originally to Zwanzig [36] and Mori [37]. These results are formal and exact. They give us relation between correlation of the "force" and correlation of dynamical variables. They are the starting point for mode-coupling theory. In the next subsections, we apply it to our chain model and introduce a series of approximations to solve it.

B. The chain model

We now apply the projection method to our chain model. We choose the normal modes as the basic quantities a_j that we are going to project out. There are several reasons for choosing the normal modes. To zeroth order approximation, each mode is nearly independent. The slowest process corresponds to long wave-length modes. The effect of short wave-length modes can be treated as stochastic noise (the random force R_t).

We choose A to be the complete set of canonical momenta and coordinates:

$$A = \begin{pmatrix} P_k^\parallel \\ P_k^\perp \\ Q_k^\parallel \\ Q_k^\perp \end{pmatrix}, \quad k = 0, 1, \cdots, N - 1, \qquad (17)$$

where

$$Q_k^\parallel = \sqrt{\frac{m}{N}} \sum_{j=0}^{N-1} u_j e^{i2\pi jk/N}, \qquad (18)$$

$$Q_k^\perp = \sqrt{\frac{m}{N}} \sum_{j=0}^{N-1} y_j e^{i2\pi jk/N}, \qquad (19)$$

$$P_k^\parallel = \dot{Q}_k^\parallel = \frac{1}{\sqrt{mN}} \sum_{j=0}^{N-1} p_{j,x} e^{i2\pi jk/N}, \qquad (20)$$

$$P_k^\perp = \dot{Q}_k^\perp = \frac{1}{\sqrt{mN}} \sum_{j=0}^{N-1} p_{j,y} e^{i2\pi jk/N}. \qquad (21)$$

We have defined the position vector $\mathbf{r}_j = (x_j, y_j) = (u_j + aj, y_j)$, so that u_j and y_j are deviations from zero-temperature equilibrium position. Because the Fourier transform is a periodic function, the index k is unique only modulo N. As a result, we can also let k vary in the range $-N/2 \leq k < N/2$. We also note that $Q_k^* = Q_{-k}$.

With these definitions, we can compute the matrix Ω and expression for the true force F in the general theory.

We find that for $\langle A, A^\dagger \rangle$, the components are

$$\langle P_k^\mu P_{k'}^{\nu\,*} \rangle = \delta_{kk'}\delta_{\mu\nu}\frac{1}{\beta}, \quad \mu,\nu = \|, \perp, \quad (22)$$

$$\langle P_k^\mu Q_{k'}^{\nu\,*} \rangle = 0, \quad (23)$$

$$\langle Q_k^\mu Q_{k'}^{\nu\,*} \rangle = \delta_{kk'}\delta_{\mu\nu}\frac{1}{\beta(\tilde{\omega}_k^\mu)^2}, \quad \beta = \frac{1}{k_B T}. \quad (24)$$

We have used equal-partition theorem for the average kinetic energy expression, and the last equation merely defines the effective frequencies $\tilde{\omega}_k^\mu$ for each mode. Note that due to translational invariance, correlation between different k modes vanishes. Correlation between transverse and longitudinal modes also vanishes due to the reflection symmetry of $y_j \to -y_j$ for the chain. Thus equal-time correlation for A is diagonal,

$$\langle A, A^\dagger \rangle = \frac{1}{\beta}\begin{pmatrix} I & 0 \\ 0 & \tilde{\omega}^{-2} \end{pmatrix}. \quad (25)$$

We have defined $\tilde{\omega}$ as a $2N \times 2N$ diagonal matrix with elements $\tilde{\omega}_k^\mu$; I is a $2N \times 2N$ identity matrix. Similarly, the correlation $\langle \dot{A}, A^\dagger \rangle$ is found from

$$\langle \dot{P}_k^\mu P_{k'}^{\nu\,*} \rangle = 0, \quad (26)$$

$$\langle \dot{P}_k^\mu Q_{k'}^{\nu\,*} \rangle = -\delta_{kk'}\delta_{\mu\nu}\frac{1}{\beta}, \quad (27)$$

$$\langle \dot{Q}_k^\mu P_{k'}^{\nu\,*} \rangle = \delta_{kk'}\delta_{\mu\nu}\frac{1}{\beta}, \quad (28)$$

$$\langle \dot{Q}_k^\mu Q_{k'}^{\nu\,*} \rangle = 0. \quad (29)$$

The second equation is from a general virial theorem [38]. We have

$$i\Omega = \langle \dot{A}, A^\dagger \rangle \langle A, A^\dagger \rangle^{-1} = \begin{pmatrix} 0 & -\tilde{\omega}^2 \\ I & 0 \end{pmatrix}. \quad (30)$$

The expression for the true force $F = \dot{A} - i\Omega A$ is then

$$F \equiv \begin{pmatrix} F^P \\ F^Q \end{pmatrix} = \begin{pmatrix} \dot{P}_k^\mu + \tilde{\omega}_k^{\mu 2} Q_k^\mu \\ 0 \end{pmatrix}. \quad (31)$$

Note that only the momentum sector has a nonzero value, and $\dot{P}_k^\mu = \ddot{Q}_k^\mu$ is given approximately by Eq. (50) and (51) below. With this special form of F, the damping matrix Γ is also diagonal and is nonzero only in the PP components. With these results, Eq. (13) becomes

$$G[z] = \begin{pmatrix} izd & -\tilde{\omega}^2 d \\ d & (iz + \tilde{\Gamma}[z])d \end{pmatrix}, \quad (32)$$

where $d = (\tilde{\omega}^2 - z^2 I + iz\tilde{\Gamma}[z])^{-1}$ is a $2N \times 2N$ diagonal matrix, and $\tilde{\Gamma}[z]$ is the Fourier-Laplace transform of the correlation $\beta\langle R_t^P, (R^P)^\dagger \rangle$, which is also diagonal (we'll denote as $\Gamma_k^\mu(t)$). In particular, we have the usual expression for the normalized coordinate correlation,

$$g_{QQ,k}^\mu(t) = \frac{\langle Q_k^\mu(t) Q_{-k}^\mu(0) \rangle}{\langle |Q_k^\mu|^2 \rangle}, \quad (33)$$

$$g_{QQ,k}^\mu[z] = \frac{iz + \Gamma_k^\mu[z]}{\tilde{\omega}_k^{\mu 2} - z^2 + iz\Gamma_k^\mu[z]}. \quad (34)$$

For simplicity, we drop the QQ subscript for the coordinate correlation for the rest of the paper.

Finally, the relation between the random force correlation and true force correlation, Eq. (16), becomes,

$$\frac{1}{\Gamma_k^\mu[z]} = \frac{1}{\Gamma_{F,k}^\mu[z]} - \frac{iz}{\tilde{\omega}_k^{\mu 2} - z^2}. \quad (35)$$

The force correlation $\Gamma_{F,k}^\mu$ can be computed from the correlation function $\beta\langle F_t^P, (F^P)^\dagger \rangle$. It is convenient to separate the linear term in the force from the nonlinear contribution. So we write

$$F^P(t) = \tilde{\omega}^2 Q(t) + \ddot{Q}(t) = (\tilde{\omega}^2 - \omega_0^2)Q(t) + f_N(t), \quad (36)$$

where $\tilde{\omega}$ is effective angular frequency and ω_0 is bare angular frequency of the mode. We have dropped the indices k and μ since these equations apply for any of the modes. f_N is at least quadratic in Q. We note that the correlation of $F^P(t)$ is linearly related to the coordinate correlation function $g[z]$,

$$\Gamma_F[z] = \frac{-iz(\tilde{\omega}^2 - z^2)}{\tilde{\omega}^2} + \frac{(\tilde{\omega}^2 - z^2)^2}{\tilde{\omega}^2}g[z]. \quad (37)$$

This is simply a consequence of Eqs. (34) and (35), but can also be derived directly from the definition. The second derivative of $Q(t)$ in frequency domain is $Q[z]$ multiplied by $(iz)^2$. Using the fact that

$$\lim_{\epsilon \to 0^+} \int_0^\infty \ddot{Q}(t)e^{-izt-\epsilon t}dt = -z^2 Q[z] - \dot{Q}(0) - izQ(0), \quad (38)$$

we can also derive Eq. (37) with the understanding that $\langle \cdots \rangle$ is an average over the initial conditions. Since $g[z]$ is finite or at least should not diverge precisely at $z = \tilde{\omega}$, this implies $\Gamma_F[\tilde{\omega}] = 0$.

With the above results, we can derive an expression of the true force correlation in terms of nonlinear force correlation,

$$\begin{aligned} \frac{\Gamma_F(t)}{\beta} &= \langle F^P(t)F^P(0)^* \rangle \\ &= \Delta\tilde{\omega}^4 \langle Q(t)Q^*(0) \rangle + \langle f_N(t)f_N(0)^* \rangle \\ &\quad - \Delta\tilde{\omega}^2\Big(\langle f_N(t)Q^*(0) \rangle + \langle Q(t)f_N^*(0) \rangle\Big), (39) \end{aligned}$$

where $\Delta\tilde{\omega}^2 = \omega_0^2 - \tilde{\omega}^2$. The mixed term can be expressed in terms of $g[z]$ by noting that $f_N = \ddot{Q} + \omega_0^2 Q$. The two mixed terms $\langle f_N(t)Q^*(0) \rangle$ and $\langle Q(t)f_N^*(0) \rangle$ are equal due to time-reversal symmetry. We find

$$\beta\tilde{\omega}^2 \int_0^\infty \langle f_N(t)Q^*(0) \rangle e^{-izt}dt = (\omega_0^2 - z^2)g[z] - iz. \quad (40)$$

Finally, we have

$$\Gamma_F[z] = \frac{\Delta\tilde{\omega}^2}{\tilde{\omega}^2}\Big((2z^2 - \omega_0^2 - \tilde{\omega}^2)g[z] + 2iz\Big) + \Gamma_N[z]. \quad (41)$$

We can also express $g[z]$ in terms of the nonlinear part of the force correlation, Γ_N $(= \beta\langle f_N(t)f_N(0)^*\rangle)$:

$$g[z] = \frac{iz(2\omega_0^2 - \tilde{\omega}^2 - z^2) + \tilde{\omega}^2\Gamma_N[z]}{(z^2 - \omega_0^2)^2}. \quad (42)$$

Again, since $g[z]$ cannot diverge precisely at $z = \omega_0$, this implies that $\Gamma_N[z]$ must take a special form to cancel the apparent divergence. Thus, if we do not take care of these superficial divergences, we will not be able to make correct prediction for the correlation function.

We can also relate the original damping function Γ to the nonlinear one,

$$\Gamma[z] = \frac{-i(\tilde{\omega}^2 - \omega_0^2)^2 z + \tilde{\omega}^2(\tilde{\omega}^2 - z^2)\Gamma_N[z]}{\omega_0^4 - \tilde{\omega}^2 z^2 - iz\tilde{\omega}^2\Gamma_N[z]}. \quad (43)$$

This last equation is useful for approximating the damping function. All of these relations are exact. This ends our formal application of the projection method to the chain model.

IV. MODE-COUPLING THEORY

To make some progress for analytic and numerical treatment, we have to make some approximations. First, we'll consider small oscillations valid at relatively low temperatures. An approximate Hamiltonian for small oscillations near zero-temperature equilibrium position, keeping only leading cubic non-linearity in the Hamiltonian, is then given by

$$H(P, Q) = \frac{1}{2}\sum_{k;\mu=\parallel,\perp}\left(P_k^\mu P_{-k}^\mu + \omega_k^{\mu 2}Q_k^\mu Q_{-k}^\mu\right)$$
$$+ \sum_{k+p+q\equiv 0 \bmod N}c_{k,p,q}Q_k^\parallel Q_p^\perp Q_q^\perp, \quad (44)$$

where

$$\omega_k^{\parallel 2} = \frac{4K_r}{m}\sin^2\frac{k\pi}{N}, \quad (45)$$

$$\omega_k^{\perp 2} = \frac{16K_\phi}{ma^2}\sin^4\frac{k\pi}{N}, \quad (46)$$

are the 'bare' dispersion relations, and

$$c_{k,p,q} = \frac{8i}{a^3 m^{3/2}N^{1/2}}\sin\frac{k\pi}{N}\sin\frac{p\pi}{N}\sin\frac{q\pi}{N}\left(\frac{1}{2}a^2 K_r\right.$$
$$\left.+K_\phi(-2 + \cos\frac{2\pi p}{N} + \cos\frac{2\pi q}{N})\right). \quad (47)$$

The absence of $Q^\parallel Q^\parallel Q^\parallel$ term in Hamiltonian (44) is due to the quadratic nature of the potential, while the absence of the terms of the form $Q^\perp Q^\perp Q^\perp$ and $Q^\parallel Q^\parallel Q^\perp$ is due to the reflective symmetry about y-axis of the Hamiltonian. We view k and $-k$ as independent component

when taking the derivatives. A slightly modified Hamilton's equation (because of the use of complex numbers) describes the dynamics:

$$\dot{P}_k^\nu = -\frac{\partial H}{\partial Q_{-k}^\nu}, \quad (48)$$

$$\dot{Q}_k^\nu = \frac{\partial H}{\partial P_{-k}^\nu}. \quad (49)$$

This gives the following equations of motion:

$$\ddot{Q}_k^\parallel = -\omega_k^{\parallel 2}Q_k^\parallel + \sum_{k'+k''=k}c_{k',k''}^{YY}Q_{k'}^\perp Q_{k''}^\perp, \quad (50)$$

$$\ddot{Q}_k^\perp = -\omega_k^{\perp 2}Q_k^\perp + \sum_{k'+k''=k}c_{k',k''}^{UY}Q_{k'}^\parallel Q_{k''}^\perp, \quad (51)$$

where

$$c_{k,p}^{YY} = i4\sqrt{\frac{1}{Nm^3a^2}}\sin\frac{k\pi}{N}\sin\frac{p\pi}{N}\sin\frac{(k+p)\pi}{N}$$
$$\left(K_r + \frac{2}{a^2}K_\phi(-2 + \cos\frac{2k\pi}{N} + \cos\frac{2p\pi}{N})\right), \quad (52)$$

$$c_{k,p}^{UY} = i8\sqrt{\frac{1}{Nm^3a^2}}\sin\frac{k\pi}{N}\sin\frac{p\pi}{N}\sin\frac{(k+p)\pi}{N}\left(K_r\right.$$
$$\left.+\frac{2}{a^2}K_\phi(-2 + \cos\frac{2p\pi}{N} + \cos\frac{2(k+p)\pi}{N})\right). \quad (53)$$

With these expressions, we are ready to compute the force correlation function in terms of dynamic variables Q_k^μ. We write

$$F_{k,\mu}^P = -\Delta\omega_k^{\mu 2}Q_k^\mu + f_{k,\mu}^N, \quad (54)$$

where $\Delta\omega_k^{\mu 2} = \omega_k^{\mu 2} - \tilde{\omega}_k^{\mu 2}$ is the difference between bare dispersion relation and effective dispersion relation. The second term $f_{k,\mu}^N$ denotes the rest of the nonlinear force (we take only the quadratic terms in Q). Due to translational and reflective symmetries, the correlation matrix formed by F^P is diagonal without any approximation. The time-displaced correlation for the diagonal terms defines true force correlation. The nonlinear part of the contributions is

$$\Gamma_{N,k}^\parallel(t) \approx \beta\sum_{k_1+k_2=k}\sum_{k_3+k_4=k}$$
$$c_{k_1,k_2}^{YY}c_{k_3,k_4}^{YY*}\langle Q_{k_1}^\perp(t)Q_{k_2}^\perp(t)Q_{k_3}^{\perp*}(0)Q_{k_4}^{\perp*}(0)\rangle, \quad (55)$$

$$\Gamma_{N,k}^\perp(t) \approx \beta\sum_{k_1+k_2=k}\sum_{k_3+k_4=k}$$
$$c_{k_1,k_2}^{UY}c_{k_3,k_4}^{UY*}\langle Q_{k_1}^\parallel(t)Q_{k_2}^\perp(t)Q_{k_3}^{\parallel*}(0)Q_{k_4}^{\perp*}(0)\rangle. \quad (56)$$

In order to have a closed system of equations for the normalized correlation functions, we use the standard mean-field type approximation, $\langle QQQQ\rangle \approx \langle QQ\rangle\langle QQ\rangle$. Owing to the δ correlation between different k, the double summation can be reduced to a single one. We introduce

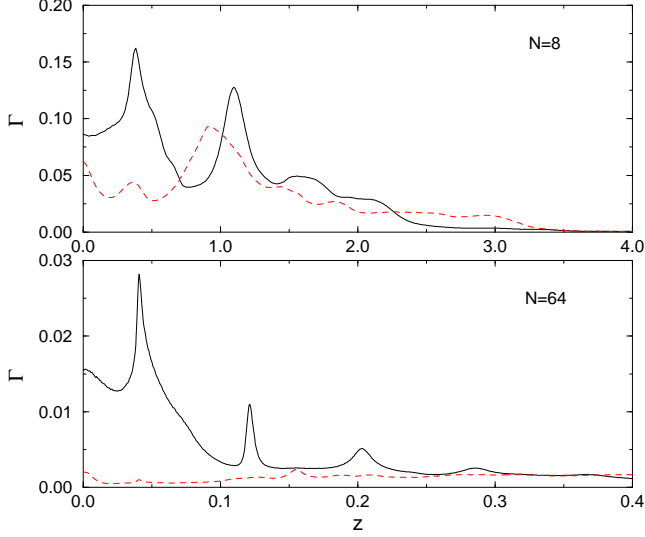$$\nu_{N,k}^\mu(t) = \Gamma_{N,k}^\mu(t)/p^2, \qquad p = \frac{2\pi k}{Na}, \quad (57)$$

FIG. 1: Damping functions of the slowest modes, i.e., real part of $\Gamma_1^{\parallel}[z]$ (solid line) and $\Gamma_1^{\perp}[z]$ (dashed line) vs z, computed from molecular dynamics for parameters of set E: $K_r = 1$, $K_\phi = 0.3$, $a = 2$, $T = 0.4$, $m = 1$. The top figure is for size $N = 8$ and bottom figure for $N = 64$.

and similarly $\nu_k^{\mu}(t)$ associated with Γ_k^{μ}. In terms of $\nu_N(t)$, we obtain

$$\nu_{N,k}^{\parallel}(t) = \sum_{k_1+k_2=k} K_{k_1,k_2}^{\parallel} g_{k_1}^{\perp}(t) g_{k_2}^{\perp}(t), \qquad (58)$$

$$\nu_{N,k}^{\perp}(t) = \sum_{k_1+k_2=k} K_{k_1,k_2}^{\perp} g_{k_1}^{\parallel}(t) g_{k_2}^{\perp}(t), \qquad (59)$$

where

$$K_{k_1,k_2}^{\parallel} = 2k_B T \left| \frac{c_{k_1,k_2}^{YY}}{\frac{2\pi(k_1+k_2)}{Na} \tilde{\omega}_{k_1}^{\perp} \tilde{\omega}_{k_2}^{\perp}} \right|^2, \qquad (60)$$

$$K_{k_1,k_2}^{\perp} = k_B T \left| \frac{c_{k_1,k_2}^{UY}}{\frac{2\pi(k_1+k_2)}{Na} \tilde{\omega}_{k_1}^{\parallel} \tilde{\omega}_{k_2}^{\perp}} \right|^2. \qquad (61)$$

Equations (58) and (59) together with the relations among $\nu_{N,k}^{\mu}$, Γ_k^{μ}, and g_k^{μ}, Eqs. (34), (43), and (57), form a system of close equations, which can be solved in principle. However, because of the singular nature at $z = \omega_0$ in Eq. (42), any approximation to Γ_N will destroy a subtle cancellation of the singularity, rendering the problem impossible to solve.

The damping function $\Gamma_k^{\mu}[z]$ is the central function that a successful theory needs to be able to calculate. In Fig. 1 we present examples of such functions determined from equilibrium molecular dynamics (MD) simulation in a microcanonical ensemble with periodic boundary condition. A more correct comparison of MD with mode-coupling theory should use an ensemble of initial conditions distributed according to canonical weight. This may be unimportant when N is large. We compute $\Gamma[z]$ from the ratio of two correlation functions,

$g_{QQ}[z]/g_{QP}[z] = iz + \Gamma[z]$. For small systems, there are a lot of peak structures associated with the low frequency modes; the feature appears washed out for large systems.

V. SOLUTION OF MODE-COUPLING THEORY

A. Numerical solution at finite N

To make the problem tractable, we make a bold approximation. Instead of Eq. (43), we take

$$\nu_k^{\mu}[z] \approx \nu_{N,k}^{\mu}[z]. \qquad (62)$$

This is equivalent to say $\tilde{\omega} \approx \omega_0$. This appears justified for the longitudinal modes at sufficiently low temperatures but problematic for the transverse mode, as $\tilde{\omega}$ is linear in wave number q but ω_0 is quadratic in q. We can consider the limit of small q. In such limit, the difference between Γ_F and Γ is dropped. Lepri's treatment [9] is similar to the above approximation. We also note that in the work of Scheipers and Schirmacher for damping of anharmonic crystals [39], effective cubic coupling is used instead of the 'bare' coupling, $c_{k,p,q}$. The standard operation of projecting the random force onto bilinear form $Q_p Q_q$ to get the mode-coupling equations also agrees with the approximation, Eq. (62), but with somewhat different "vertex functions" replacing Eq. (60) and (61).

In order to obtain a numerical solution, besides the model parameters (mass m, lattice spacing a, couplings K_r and K_ϕ), we also need the effective dispersion relation. We used MD data for this purpose. It turns out that a two-parameter fit of the form

$$\tilde{\omega}_k = \frac{2c}{a} \left| \sin \frac{k\pi}{N} \right| + \left(\omega_{\max} - \frac{2c}{a} \right) \sin^2 \frac{k\pi}{N} \qquad (63)$$

characterizes the effective dispersion relation very well, where c is sound velocity at small k and $\omega_{\max}$ is maximum frequency at $k = N/2$.

We used a fast Fourier transform to solve the equations iteratively. Given an initial $\nu[z]$, correlation function in frequency domain is calculated by Eq. (34). Inverse transform gives us $g(t)$, which is used to calculate the discrete sum in Eqs. (58) and (59) to obtain $\nu(t)$. We transform back to frequency domain for the next iteration.

Figure 2 is our theoretical calculation with parameters exactly at set E. This figure should be compared with the MD data in Fig. 1. We observe that the predicted results are too smooth without much structure. The mode-coupling theory predicts a damping that is a factor of two larger for the longitudinal modes and much too large for the transverse modes. By adjusting the temperature to a lower value (one half for $N = 8$ and a quarter for $N = 64$), we obtain curves which closely resemble the MD results. However, the mode-coupling
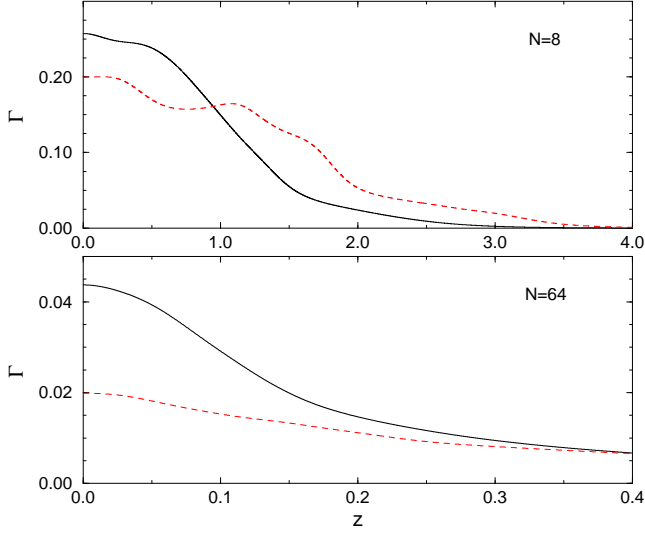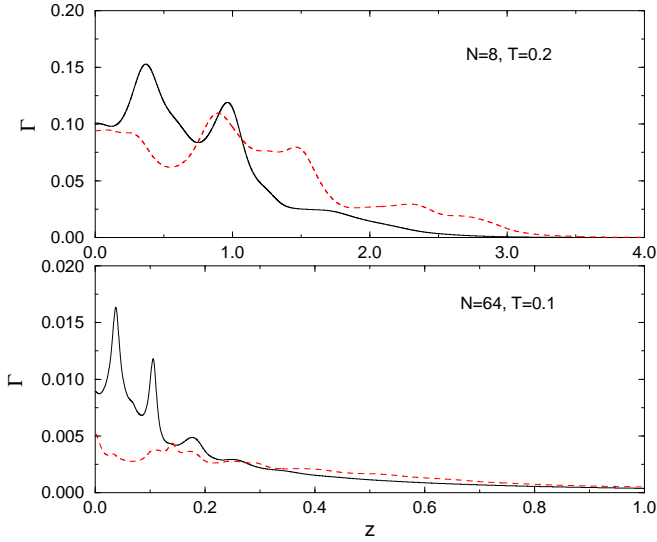
FIG. 2: Real part of $\Gamma_1^{\parallel}[z]$ (solid line) and $\Gamma_1^{\perp}[z]$ (dashed line) vs z from a full mode-coupling theory for parameters of set E (same as that in Fig.1) at $N = 8$ and 64. The input effective dispersion relation parameters, $c^{\parallel}, c^{\perp}, \omega_{\max}^{\parallel}$, and $\omega_{\max}^{\perp}$, are given in Table I.

FIG. 3: Real part of $\Gamma_1^{\parallel}[z]$ (solid line) and $\Gamma_1^{\perp}[z]$ (dashed line) vs z from a full mode-coupling theory for parameters of set E, but at different temperature T. Other parameters are the same as in Fig. 2.

theory still overestimates the value of transverse damping. It is clear that $K^{\perp}$ is considerably smaller in actually system, but our mode-coupling theory can not produce a small enough $K^{\perp}$.

TABLE I: Parameters for mode-coupling equations.

Set E	bare	$N = 8$	$N = 64$	$N = 1024$
$c^{\parallel}$	2	1.435	1.341	1.329
$c^{\perp}$	0	0.621	0.669	0.674
$\omega_{max}^{\parallel}$	2	1.495	1.543	1.553
$\omega_{max}^{\perp}$	1.095	1.087	1.182	1.194
v_0	2	0.7113	0.6333	0.6337
v_1	0	-0.1060	-0.0221	-0.0076
v_2	-0.6	-0.1099	-0.1242	-0.1293
v_3	0	0.6362	0.8965	0.9312
v_4	0	-0.0424	-0.1346	-0.1469

B. An effective Hamiltonian approach

The results presented in Fig. 3 give us some hints that the mode-coupling equations are essentially correct, but the parameters of the model need to be adjusted. In fact, simple perturbative expansion of the Hamiltonian can not correctly predict $\tilde{\omega}_k^{\perp}$. According to MD result, $\tilde{\omega}_k^{\perp} \propto k$, but the leading contribution from perturbation calculation should give the 'bare' frequency, $\tilde{\omega}_k^{\perp} = \omega_k^{\perp} \propto k^2$.

The adjusting of the parameters can be made more rigorous [39] with an introduction of an effective Hamiltonian,

$$
\begin{aligned}
\tilde{H}(P,Q) &= \frac{1}{2} \sum_{k,\mu=\parallel,\perp} \left(P_k^{\mu} P_{-k}^{\mu} + (\tilde{\omega}_k^{\mu})^2 Q_k^{\mu} Q_{-k}^{\mu} \right) \\
&+ \sum_{k+p+q=0} \tilde{V}_{kpq} Q_k^{\parallel} Q_p^{\perp} Q_q^{\perp} + \sum_{k+p+q=0} \tilde{V}_{kpq}^{(3)} Q_k^{\parallel} Q_p^{\parallel} Q_q^{\parallel} \\
&= H^0 + H'.
\end{aligned}
\tag{64}
$$

The form of the Hamiltonian is dictated by symmetry. Translational invariance requires that $k + p + q = 0$ (mod N). The system is symmetric under reflection about y-axis or x-axis. Thus the Hamiltonian should be invariant under the transformation $Q_k^{\perp} \to -Q_k^{\perp}$ or $Q_k^{\parallel} \to -Q_{-k}^{\parallel}$. In addition, $\tilde{V}_{kpq}$ is symmetric under permutation of p and q, and $\tilde{V}_{kpq}^{(3)}$ is symmetric under permutation of all three indices. We also have $\tilde{V}_{-k,-p,-q} = -\tilde{V}_{k,p,q}$ and similarly for $\tilde{V}_{kpq}^{(3)}$. Although the original Hamiltonian does not have $V^{(3)}$ term, such a term can present. One of the reasons that such term can present is due to the non-analytic behavior of the potential (because of the absolute value $|\cdot|$).

We determine the parameters of the effective Hamiltonian, $\tilde{\omega}_k^{\parallel}, \tilde{\omega}_k^{\perp}, \tilde{V}$, and $\tilde{V}^{(3)}$, by fitting them to the observed time-independent correlation functions from MD. In order to be able to carry out the calculation analytically, we treat the interactions as perturbations, i.e., $\tilde{V}$ and $\tilde{V}^{(3)}$ are assumed small. All the equilibrium averages are approximated by the leading contribution from

the perturbation,

$$\langle \cdots \rangle \approx \langle \cdots (1 - \beta H') \rangle_0 \qquad (65)$$

where $\langle \cdots \rangle_0$ is thermodynamical average with respect to the non-interacting harmonic oscillators (product of Gaussian integrals). Under the above approximation, we find

$$\langle |Q_k^\mu|^2 \rangle = \frac{1}{\beta(\tilde{\omega}_k^\mu)^2} + O(\tilde{V}^2), \qquad (66)$$

and the interaction parameters

$$\tilde{V}_{kpq} = \frac{\langle Q_k^\| Q_p^\perp Q_q^\perp \rangle}{2\beta \langle |Q_k^\||^2 \rangle \langle |Q_p^\perp|^2 \rangle \langle |Q_q^\perp|^2 \rangle}, \qquad (67)$$

$$\tilde{V}_{kpq}^{(3)} = \frac{\langle Q_k^\| Q_p^\| Q_q^\| \rangle}{6\beta \langle |Q_k^\||^2 \rangle \langle |Q_p^\||^2 \rangle \langle |Q_q^\||^2 \rangle}. \qquad (68)$$

The actual form of the $\tilde{\omega}$ is fitted according to Eq. (63). For $\tilde{V}$ and $\tilde{V}^{(3)}$ we fit into a functional form

$$\tilde{V}_{kpq} = \frac{ixyz}{\sqrt{N}} \left(v_0 + v_1 z^2 + v_2 (x^2 + y^2) \right), \qquad (69)$$

$$\tilde{V}_{kpq}^{(3)} = \frac{ixyz}{\sqrt{N}} \left(v_3 + v_4 (x^2 + y^2 + z^2) \right), \qquad (70)$$

where $z = \sin(k\pi/N)$, $x = \sin(p\pi/N)$, and $y = \sin(q\pi/N)$. The values of v_0 to v_4, together with c and ω_{max} are listed in Table I. It is surprising that not only is the $\tilde{V}^{(3)}$ term present, but also is its magnitude comparable to $\tilde{V}$. The column marked 'bare' are the parameters corresponding to the 'bare' Hamiltonian, Eq. (44). The bare parameters are reached only at very low temperatures, such as $T = 0.002$. Since we have factored out the leading size dependence, we expect the parameters weakly depending on size N.

Before presenting our results with the effective parameters, it is worth pointing out that the standard procedure of deriving mode-coupling equations gives identical result as our approximation, Eq. (62). The standard procedure is to project the random force, $R_k = \tilde{\omega}_k^2 Q_k + \ddot{Q}_k$, onto a bilinear form of the basic variable Q_k. Applying the general projection operator, Eq. (5), to our case, this bilinear projector is

$$\mathcal{P}_2 f = \sum_{i \neq j, i \leq j} \langle f Q_i^* Q_j^* \rangle \frac{Q_i Q_j}{\langle |Q_i Q_j|^2 \rangle} + \sum_i N_i Q_i Q_{\bar{i}}, \quad (71)$$

where i or j is a pair of indices, e.g., $j = (k, \mu)$, and $\bar{j}$ is $(-k, \mu)$. In evaluating the four-point correlation functions, we have neglected the perturbation term. It turns out that the last term projects out only the $k = 0$ component. Thus, the specific values of N_i are not needed.

After applying projector $\mathcal{P}_2$ onto R_k^μ, we neglect the difference between normal dynamics $e^{t\mathcal{L}}$ and anomalous dynamics for $R_k^\mu(t)$, $e^{t\mathcal{P}'\mathcal{L}}$. We have

$$\Gamma_k^\mu(t) = \beta \langle R_k^\mu(t) R_k^\mu(0)^* \rangle$$
$$\approx \beta \left\langle \left(e^{t\mathcal{L}} \mathcal{P}_2 R_k^\mu(0) \right) \left(\mathcal{P}_2 R_k^\mu(0) \right)^* \right\rangle. \qquad (72)$$
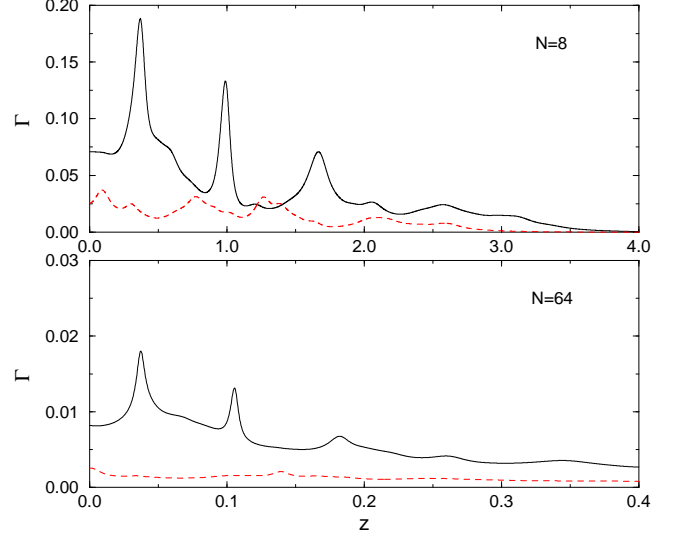

FIG. 4: Real part of $\Gamma_1^\|[z]$ (solid line) and $\Gamma_1^\perp[z]$ (dashed line) vs z from a full mode-coupling theory for set E, using effective parameters given in Table I.

The mode-coupling equations are then,

$$\Gamma_k^\|(t) = \sum_{p+q=k} \left(\tilde{K}_{pq}^\| g_p^\perp(t) g_q^\perp(t) + \tilde{K}_{pq}^{(3)} g_p^\|(t) g_q^\|(t) \right), (73)$$

$$\Gamma_k^\perp(t) = \sum_{p+q=k} \tilde{K}_{pq}^\perp g_p^\|(t) g_q^\perp(t), \qquad (74)$$

where

$$\tilde{K}_{pq}^\| = \frac{\beta}{2} \frac{|\langle R_{p+q}^\| Q_{-p}^\perp Q_{-q}^\perp \rangle|^2}{\langle |Q_p^\perp|^2 \rangle \langle |Q_q^\perp|^2 \rangle} = \frac{2}{\beta} \left| \frac{\tilde{V}_{-p-q,p,q}}{\tilde{\omega}_p^\perp \tilde{\omega}_q^\perp} \right|^2, (75)$$

$$\tilde{K}_{pq}^\perp = \beta \frac{|\langle R_{p+q}^\perp Q_{-p}^\| Q_{-q}^\perp \rangle|^2}{\langle |Q_p^\||^2 \rangle \langle |Q_q^\perp|^2 \rangle} = \frac{4}{\beta} \left| \frac{\tilde{V}_{p,-p-q,q}}{\tilde{\omega}_p^\| \tilde{\omega}_q^\perp} \right|^2, (76)$$

$$\tilde{K}_{pq}^{(3)} = \frac{\beta}{2} \frac{|\langle R_{p+q}^\| Q_{-p}^\| Q_{-q}^\| \rangle|^2}{\langle |Q_p^\||^2 \rangle \langle |Q_q^\||^2 \rangle} = \frac{18}{\beta} \left| \frac{\tilde{V}_{-p-q,p,q}^{(3)}}{\tilde{\omega}_p^\| \tilde{\omega}_q^\|} \right|^2. (77)$$

Note that the vertex coupling $\langle R_k Q_p Q_q \rangle = \tilde{\omega}^2 \langle Q_k Q_p Q_q \rangle$ is proportional to the three-point correlation independent of the specific form of random force. This version of mode-coupling equation need not have the limitation of small oscillations, and can be applied to high temperatures as well.

Figure 4 is a calculation of the real part of $\Gamma_k^\mu[z]$ for $k = 1$. Comparing with Fig. 2 and 3, we see that using effective parameters brings into much better agreement with the MD data. In fact, comparing to Fig. 1, most of the features are reproduced, such as the locations and heights of the peaks. The most important improvement is the ratio of parallel to perpendicular damping.

In Figure 5, we compare the normalized dynamic correlation functions for size $N = 256$ and the slowest mode
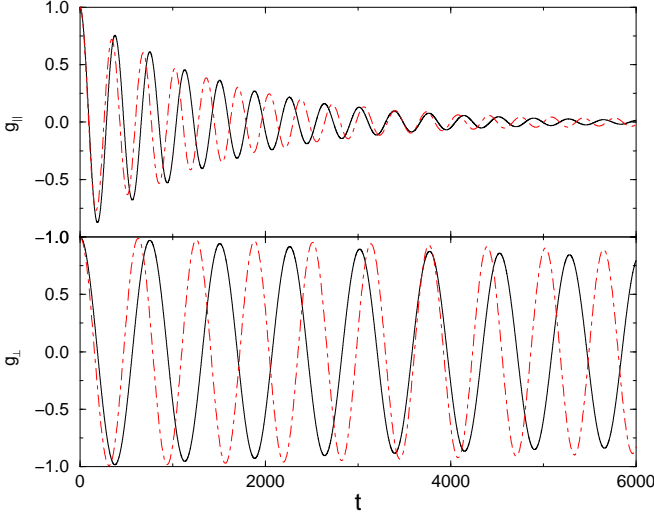
FIG. 5: The normalized correlation functions $g_1^\parallel(t)$ (upper part) and $g_1^\perp(t)$ (lower part) on a $N = 256$ system for data set E. The solid curves are from full mode-coupling theory, while the dotted dashes are from equilibrium molecular dynamics.

FIG. 6: The decay rate γ_k for each mode k for system size $N = 1024$. Circles ($\gamma_k^\parallel$) and triangles ($\gamma_k^\perp$) are from molecular dynamics by fitting the correlation function, while the continuous curves are from a full mode-coupling theory for set E, using effective parameters given in Table I.

$k = 1$. The frequencies of oscillations are slightly different in MD and mode-coupling calculation, thus there are phase shifts at long times. The longitudinal damping agrees with each other extremely well. A fit of the logarithm of amplitudes (maxima and minima) versus time for the MD data gives the decay rate $\gamma_1^\parallel \approx 0.00064$, $\gamma_1^\perp \approx 0.000023$, while mode-coupling predicts $\gamma_1^\parallel \approx 0.00066$ and $\gamma_1^\perp \approx 0.000078$, respectively. Mode-coupling theory with effective parameters still overestimates the transverse damping by a factor of 2 to 3.

In Fig. 6, we show the damping of the mode in terms of the decay constant γ_k, which is defined by the exponential decay in $g(t) \approx \cos(\tilde{\omega}_k t)e^{-\gamma_k t}$. The symbols are obtained from MD simulation, while the curves are from the full mode-coupling theory with effective parameters. For MD data, γ_k is obtained by a least-square fit to the amplitudes. For mode-coupling theory, we use an approximation, $\gamma_k = \frac{1}{2}\bar{\Gamma}_k[\tilde{\omega}_k]$. The bar means we average over a window centered around $\tilde{\omega}_k$ with width about γ_k. We observe that excellent agreement between MD data and mode-coupling theory is obtained for the parallel component. The mode-coupling theory overestimates the transverse mode damping by some constant factor. In any case, the slopes of the curves agree very well with the expected results (to be discussed in the next subsection), $\gamma_k^\parallel \propto k^{3/2}$ and $\gamma_k^\perp \propto k^2$.

C. Large N limit

To simplify the equations further, we consider the large size limit. Since the large size asymptotic behavior is the most interesting, such limiting results are justified. We
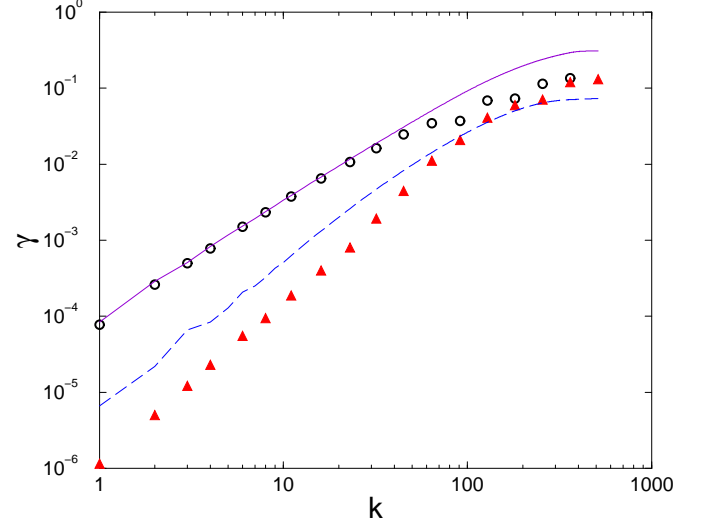
thus consider the limit of $p \to 0$ and keep only leading contributions in lattice momentum $p = 2\pi k/(Na)$. In this limit the three kernel functions K_{k_1,k_2}^μ become constants. In addition, we define a k-independent ν function by taking the limit $p \to 0$. The leading k-dependence in Γ_k is k^2. When this term is factored out, we expect that ν_k becomes independent of k in the limit of large N and small p. With these simplification and approximation, and converting the discrete summation to integral, we have in the limit of large sizes:

$$\nu^\parallel(t) = \frac{1}{2\pi}\int_{-\pi/a}^{\pi/a}dq\,\left(K^\parallel g_q^\perp(t)^2 + K^{(3)}g_q^\parallel(t)^2\right),\quad(78)$$

$$\nu^\perp(t) = \frac{K^\perp}{2\pi}\int_{-\pi/a}^{\pi/a}dq\,g_q^\parallel(t)g_q^\perp(t),\quad(79)$$

where

$$K^\parallel = \frac{a^5 K_r^2}{2\beta c^{\perp 4}m^3},\ K^{(3)} = 0,\ K^\perp = \frac{a^5 K_r^2}{\beta c^{\parallel 2}c^{\perp 2}m^3},\quad(80)$$

if we use the perturbation expansion Hamiltonian, or

$$K^\parallel = 4\left(\frac{a}{2}\right)^7\frac{v_0^2}{\beta c^{\perp 4}},\quad K^{(3)} = 36\left(\frac{a}{2}\right)^7\frac{v_3^2}{\beta c^{\parallel 4}},$$

$$K^\perp = 8\left(\frac{a}{2}\right)^7\frac{v_0^2}{\beta c^{\parallel 2}c^{\perp 2}},\quad(81)$$

if we use the effective Hamiltonian. We also linearize the dispersion relation so that $\omega_p^\mu = c^\mu p$, $c^\mu = c^\parallel$ or $c^\perp$ are effective sound velocities for the longitudinal and transverse modes.

We shall refer to Eqs. (78) and (79) as simple mode-coupling theory and the finite N version as the full mode-coupling theory.

D. Asymptotic analytic solution

Assuming that the simplified mode-coupling equations represent the essence of the physics regarding the damping and time-dependent correlation functions, we now consider analytic solution to Eqs. (78) and (79). First we notice some constraints on the functions. Because $\nu^\mu(t)$ is a real function, we must have $\nu[z]^* = \nu[-z]$. Since $g_q^\mu(0) = 1$, we must have $\nu^\mu(0) = K^\mu/a$, for $\nu = \parallel$ or $\perp$ (assuming $K^{(3)} = 0$). This implies that the Fourier-Laplace transform must be integrable:

$$\nu(0) = \frac{1}{\pi} \int_{-\infty}^{\infty} \nu[z]\,dz = \frac{K}{a}. \qquad (82)$$

Next, the large z behavior can be obtained by integrating by part few times, using the boundary conditions $g(0) = 1$, $g'(0) = 0$, $g''(0) = -\tilde\omega^2$, and $g(t \to \infty) = 0$. For simplicity, we have omitted the lattice momentum index q and mode index $\parallel$ or $\perp$, since it is true for any g_q^μ. With these results, we find

$$
\begin{aligned}
\nu[z] &= \int_0^\infty \nu(t)\,e^{-izt}dt \\
&= \frac{K}{2\pi} \int_{-\pi/a}^{\pi/a} dq \int_0^\infty g_q^1(t)\,g_q^2(t)\,e^{-izt}dt \\
&= \frac{K}{iaz} + \frac{K}{2\pi i z^3} \int_{-\pi/a}^{\pi/a} dq(\tilde\omega_1^2 + \tilde\omega_2^2) + O\left(\frac{1}{z^5}\right), \ (83)
\end{aligned}
$$

where for $\nu^\parallel$, g^1 and g^2 are all $g^\perp$, while for $\nu^\perp$, it is $g^\parallel$ and $g^\perp$.

We can establish that

$$\nu^\parallel[z] \propto (iz)^{-1/2}, \quad \nu^\perp[z] \propto \text{const}, \qquad (84)$$

in the limit of small $K^\perp$. We proceed as follows: first we assume that $\nu^\perp[z] = \nu_0^\perp$ or $\nu^\perp(t) = 2\nu_0^\perp\delta(t)$. We then derive an expression for $\nu^\parallel(t)$ and $\nu^\perp(t)$, and show that indeed $\nu^\perp(t)$ approaches a δ-function in a proper limit.

When $\nu^\perp[z]$ is a constant, the inverse Fourier transform for the correlation function $g[z]$ can be performed exactly, to give the transverse correlation function as

$$
\begin{aligned}
g_q^\perp(t) =\ & \frac{1}{2}\left(1 + \frac{\Gamma_q^\perp}{2i\bar\omega}\right) e^{i\bar\omega t - \frac{1}{2}\Gamma_q^\perp t} + \\
& \frac{1}{2}\left(1 - \frac{\Gamma_q^\perp}{2i\bar\omega}\right) e^{-i\bar\omega t - \frac{1}{2}\Gamma_q^\perp t}, \qquad (85)
\end{aligned}
$$

where $\Gamma_q^\perp = \nu_0^\perp q^2$, and $\bar\omega = \sqrt{c^{\perp 2}q^2 - \Gamma_q^{\perp 2}/4} \approx c^\perp q$. We have linearized the dispersion relation, $\tilde\omega \approx c^\perp q$. We

only look at the dominant term in time dependence of $\nu^\parallel(t)$. For $g_q^\perp(t)^2$, since large q-mode decays rapidly, we ignore the term with amplitude proportional to q^2, and also drop the oscillatory term and approximate, $g_q^\perp(t)^2 \approx \frac{1}{2}e^{-\Gamma_q^\perp t}$. After integrating over q (we also extend the limit as from $-\infty$ to ∞), we obtain the leading t dependence, as

$$\nu^\parallel(t) \approx \frac{K^\parallel}{4}\sqrt{\frac{1}{\pi\nu_0^\perp t}}. \qquad (86)$$

If the oscillatory terms are kept, they only contribute an exponentially small term, $e^{-(c^\perp)^2 t/\nu_0^\perp}$; and the q^2 terms give a contribution that decays much faster, as $t^{-3/2}$. The contribution from $K^{(3)}$ term can be neglected, because it decays as $t^{-2/3}$ (due to Eq. (91)). But this term does provide a crossover from $z^{-1/3}$ for intermediate z to the asymptotic $z^{-1/2}$ for very small z. The Fourier-Laplace transform gives

$$\nu^\parallel[z] \approx \frac{K^\parallel}{4}\sqrt{\frac{1}{i\nu_0^\perp z}} = b(iz)^{-1/2}. \qquad (87)$$

We now get an expression for the longitudinal correlation function. Formally, it is given by the inverse transform

$$g_q^\parallel(t) = \frac{1}{2\pi} \int_{-\infty}^{\infty} \frac{-iz - \Gamma_q^\parallel[z]}{z^2 - c^{\parallel 2}q^2 - iz\Gamma_q^\parallel[z]} e^{izt}dz, \qquad (88)$$

where $\Gamma_q^\parallel[z] = q^2\nu^\parallel[z] = bq^2/\sqrt{iz}$, $b = \frac{1}{4}K^\parallel/\sqrt{\nu_0^\perp}$. The dominant contribution is from z when the denominator is close to zero. The integral can be approximately estimated by the residue theorem. By location the poles

$$z^2 - c^{\parallel 2}q^2 - \sqrt{iz}\,b\,q^2 = 0, \qquad (89)$$

we obtain the dispersion relation for $g_q^\parallel(t)$. In the limit of small q, we find

$$z \approx c^\parallel q + i\gamma_0 q^{3/2}, \qquad (90)$$

where $\gamma_0 = \frac{\sqrt{2}}{16}K^\parallel/\sqrt{c^\parallel \nu_0^\perp}$. Therefore,

$$g_q^\parallel(t) \approx e^{-\gamma_0 q^{3/2}t}\cos(c^\parallel q t). \qquad (91)$$

Similarly with the dispersion relation for the transverse mode, $z \approx c^\perp q + \frac{1}{2}i\nu_0 q^2$, we can compute

$$
\begin{aligned}
\nu^\perp(t) =\ & \frac{K^\perp}{\pi} \int_0^\infty dq\, e^{-\gamma_0 q^{3/2}t - \frac{1}{2}\nu_0^\perp q^2 t}\cos(c^\parallel q t)\cos(c^\perp q t) \\
\approx\ & K^\perp \sqrt{\frac{1}{8\pi\nu_0^\perp t}}\left(e^{-\frac{(c^\parallel - c^\perp)^2}{2\nu_0}t} + e^{-\frac{(c^\parallel + c^\perp)^2}{2\nu_0}t}\right). \ (92)
\end{aligned}
$$

We have neglected the γ_0 term. Since $|c^\parallel - c^\perp|$ is smaller than $c^\parallel + c^\perp$, we drop the second term. We symmetrically

extend the function. Note that $\nu^\perp(t)$ can be casted into the functional form

$$f_\sigma(t) = \frac{1}{2}\sqrt{\frac{\sigma}{\pi}}\frac{e^{-\sigma|t|}}{\sqrt{|t|}}, \quad \sigma = \frac{(c^\parallel - c^\perp)^2}{2\nu_0^\perp}, \qquad (93)$$

which has the property that

$$\int_{-\infty}^{\infty} f_\sigma(t)\,dt = 1, \quad \text{for all} \quad \sigma > 0. \qquad (94)$$

Thus $f_\sigma(t)$ behaves as a δ-function as $\sigma \to \infty$:

$$\nu^\perp(t) \approx \frac{K^\perp}{|c^\parallel - c^\perp|}\delta(t). \qquad (95)$$

This allows us to identify the constant $\nu_0^\perp = \frac{1}{2}K^\perp/|c^\parallel - c^\perp|$. The condition for $\sigma \to \infty$ is the same as $\nu_0^\perp \to 0$ or $K^\perp \to 0$. Since $K^\perp/K^\parallel = 2(c^\perp/c^\parallel)^2$ (c.f. Eq.(80)), small $K^\perp$ also implies small $c^\perp$.

Although the above derivation suggests that the result is valid only for the special limit. But in fact, this is also the asymptotic result in the limit $z \to 0$. To show this, we note that the asymptotic behavior is picked up by the scaling $\lim_{\lambda \to 0} \lambda^\delta \nu[\lambda z] \approx \nu[z]$. If this is true, then $\nu[z] \propto z^{-\delta}$. This scaling limit coincides with the limit of $K^\perp \to 0$.

E. Numerical solution of the simple theory

For the simple mode-coupling theory that we have already taken the large N limit, we can also apply the fast Fourier transform method. However, we find that a direct numerical integration in frequency space is much more accurate. For example, $\nu^\perp[z]$ is expressed as

$$\nu^\perp[z] = \frac{K^\perp}{(2\pi)^3}\int_{-\infty}^{+\infty}d\omega\int_{-\infty}^{+\infty}d\omega'\,2\,F_\perp(\omega,\omega')$$
$$\left(\mathrm{P}\frac{1}{i(z-\omega-\omega')} + \pi\delta(z-\omega-\omega')\right), (96)$$

where P stands for Cauchy principal value and

$$F^\perp(\omega,\omega') = \int_0^{\pi/a} g^\parallel(q,\omega)g^\perp(q,\omega')\,dq, \qquad (97)$$

$$g^{\parallel,\perp}(q,\omega) = \frac{-i\omega - \nu^{\parallel,\perp}[\omega]q^2}{\omega^2 - (c^{\parallel,\perp})^2q^2 - i\omega\nu^{\parallel,\perp}[\omega]q^2}. \qquad (98)$$

When the linear approximation is made to the dispersion relations, the integral over q can be performed analytically. We only need to do a two-dimensional integral over ω and ω'. The principal value integral is taken care by locating exactly the singularity. Since the integration routine needs a smooth function $\nu[z]$, we fit the results by a Padé approximation (in variable iz or $(iz)^{1/3}$). The procedure is iterated several times for convergence. This is programmed in *Mathematica*. It turns out essential to
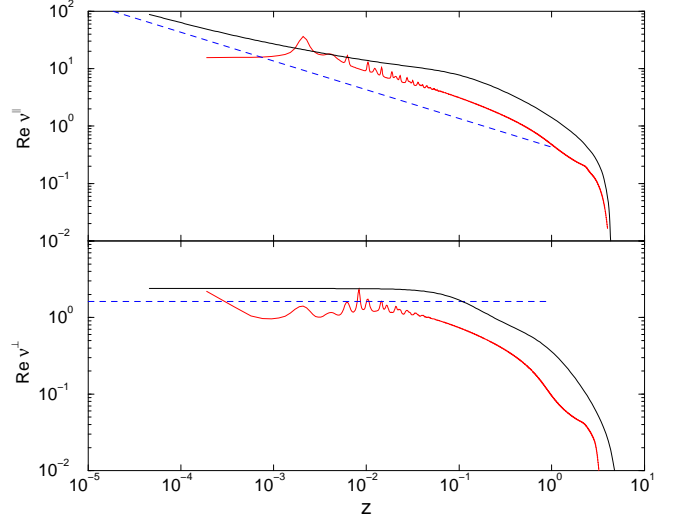

FIG. 7: Real part of $\nu^\parallel[z]$ (top) and $\nu^\perp[z]$ (bottom) for data set E. The smooth curves are from simple mode-coupling theory, the (red) curves with spikes are computed from full theory at $N = 1024$, while the straight, dash lines are analytic asymptotic results.
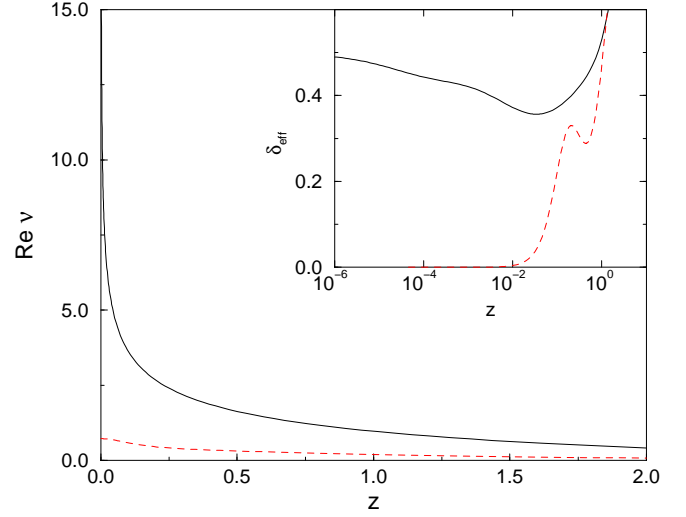

FIG. 8: Real part of $\nu^\parallel[z]$ (solid line) and $\nu^\perp[z]$ (dashed line) for data set J ($K^\parallel = 1.532$, $K^\perp = 0.719$, and $K^{(3)} = 2.776$). The insert shows the effective exponent $-d\ln\nu/d\ln z$.

have more than double precision accuracy in the integration routine in order for the singular integrals properly converged. Some results of this calculation are already presented in ref. [31].

In Fig. 7, we compare three levels of approximations of $\nu^\mu[z]$: the simple mode-coupling theory, the full theory computed on $N = 1024$ by $\nu^\mu[z] = \Gamma_1^\mu[z]/(2\pi/(Na))^2$, and the asymptotic result of $\nu^\perp[z] = \frac{1}{2}K^\perp\big(1/|c^\parallel - c^\perp| + 1/|c^\parallel + c^\perp|\big)$, and Eq. (87). Noticeable differences are seen between full theory and simplified. This is partly due to
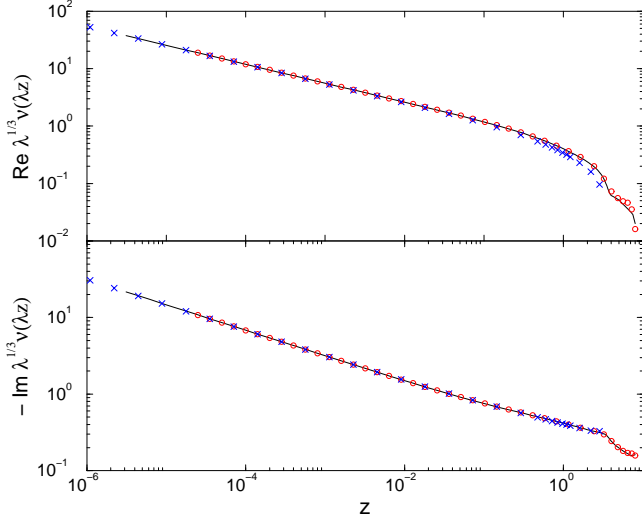
FIG. 9: Real part (top) and imaginary part (bottom) of $\lambda^{1/3}\nu(\lambda z; K, \lambda^{1/3}c, \lambda^{-2/3}a)$ vs z for $K = c = a = 1$ and $\lambda = 1$ (solid line), $1/8$ (open circles), and 8 (crosses).

the fact that we are comparing a finite N with an infinite N result. We also note that the asymptotic slope of $-1/2$ for $\nu^{\|}[z]$ is approached rather slowly.

Figure 8 shows a stronger crossover effect from slope of $1/3$ (corresponding to $\kappa \propto N^{2/5}$, to be discussed later) to that of the true asymptotic law of $1/2$. This set of curves corresponds to data set J.

F. Scaling solution of the simple theory

We now look at some of the scaling properties that are implied from Eqs. (78) and (79). First, we consider the simple case of $K = K^{\|} = K^{\perp}$, $K^{(3)} = 0$, and $c = c^{\|} = c^{\perp}$. In this case the two equations degenerate into one equation given by Lepri [9]. By measuring frequency in terms of c (i.e., consider variable z/c) we can scale away c, thus the following equation is an exact scaling

$$\nu(z; K, c, a) = c\,\nu(z/c; K/c^2, 1, a), \qquad (99)$$

where ν is a function of z with parameters K, c, and a that we have written out explicitly. This equation tells us that out of the three parameters that characterize the solution, we can pick two as independent. The "shapes" of the solutions are all the same for $K/c^2 = $ const. Without loss of generality, we can fix $K = 1$.

Next, we consider a general scaling solution of the form

$$\nu(\lambda z; K, \lambda^{\Delta_c}c, \lambda^{\Delta_a}a) \approx \lambda^{-\delta}\nu(z; K, c, a). \qquad (100)$$

Substituting this scaling form into Eq. (96), by requiring that the result must be consistent, we obtain the follow-

ing conditions

$$2\Delta_q - \delta - 1 = 0, \qquad (101)$$
$$\Delta_c + \Delta_q - 1 = 0, \qquad (102)$$
$$1 - \Delta_q = \delta, \qquad (103)$$
$$\Delta_a + \Delta_q = 0, \qquad (104)$$

where Δ_q is scaling exponent associated with integration variable q, $q \to \lambda^{\Delta_q}q$. A unique solution to the set of linear equations is obtained, $\delta = 1/3$, $\Delta_c = 1/3$, $\Delta_a = -2/3$, and $\Delta_q = 2/3$. Since Eq. (100) is (approximately) valid for any λ, we can choose $\lambda = 1/z$. This scaling solution implies that

$$\nu(z; K, c, a) \approx z^{-1/3}\nu(1; K, c/z^{1/3}, z^{2/3}a). \qquad (105)$$

Power-law behavior $z^{-1/3}$ is obtained in the limit of small z, relatively large c, and small a, if $\nu(1, K, \infty, 0)$ is finite. The crossover to other behavior occurs at large $z \sim c^3$ and $z \sim a^{-3/2}$.

A simple dimension analysis also leads to the $z^{-1/3}$ factor. Let the dimension of length and time be L and T, respectively. Then the dimensions of relevant quantities are $[z] = T^{-1}$, $[c] = LT^{-1}$, $[a] = L$, $[\nu] = L^2 T^{-1}$, and $[K] = L^3 T^{-2}$. From the five quantities, we can construct three dimensionless variables

$$\Pi_1 = \frac{\nu}{z^{-1/3}K^{2/3}}, \quad \Pi_2 = \frac{c}{z\,a}, \quad \Pi_3 = \frac{K}{ac^2}. \qquad (106)$$

If there is any relation between the Π_i's, it must be in the form $\Pi_1 = f(\Pi_2, \Pi_3)$ (Buckingham Pi theorem [40]), or

$$\nu[z] = z^{-1/3}K^{2/3}f\left(\frac{za}{c}, \frac{K}{ac^2}\right), \qquad (107)$$

where f is an arbitrary, dimensionless function. This result, of course, is consistent with Eq. (100). This also suggests that the scaling is not approximate, but an exact result.

Fig. 9 is a test of the above scaling by numerical solutions. For small z, the power-law $z^{-1/3}$ is verified to high accuracy. Since this scaling is exact, the deviations are due purely to numerical errors in solving the equations.

The case of the coupled longitudinal and transverse equations is somewhat difficult to analyze. We can require a very general scaling of the form

$$\nu^{\|}(\lambda z; \lambda^{\Delta_{K^{\|}}}K^{\|}, \lambda^{\Delta_{K^{\perp}}}K^{\perp}, \lambda^{\Delta_{c^{\|}}}c^{\|}, \lambda^{\Delta_{c^{\perp}}}c^{\perp}, \lambda^{\Delta_a}a)$$
$$\approx \lambda^{-\delta_{\|}}\nu(z; K^{\|}, K^{\perp}, c^{\|}, c^{\perp}, a), \quad (108)$$

and similarly for the perpendicular component. If we require for consistency of scaling for both longitudinal and transverse components, we find that the only scaling solution is the symmetric solution, i.e., the scaling discussed above with identical longitudinal and transverse scaling exponents.

If we abandon the exact scaling for the transverse component and look only at longitudinal component, we can require that

$$\delta_\perp = 2\Delta_q - 1, \tag{109}$$
$$\delta_\parallel = 1 - \Delta_{K\parallel} - \Delta_q, \tag{110}$$
$$\Delta_{c\perp} = 1 - \Delta_q. \tag{111}$$

As before we can require that there is no scaling for the coupling constant $K^\parallel$ without loss of generality (i.e., $\Delta_{K\parallel} = 0$), the above equations imply a relation

$$2\delta_\parallel + \delta_\perp = 1. \tag{112}$$

In particular, if $\delta_\perp = 0$, we must have $\delta_\parallel = 1/2$ and $\Delta_{c\perp} = 1/2$. This is consistent with the fact that the scaling region of $\delta_\parallel = 1/2$ is obtained for small $c^\perp$.

A complete and clear scaling picture is still lacking. From the numerical solution, we observe that besides well characterized scaling regimes, there are also plenty of intermediate regions and crossovers. For very large $c^\perp$ and small $K^\perp$, or small $c^\perp$ and large $K^\perp$, the behavior of the solutions are difficult to characterize.

VI. GREEN-KUBO FORMULA

In this section, we make the connection of the damping of modes with thermal conduction. The starting point is the Green-Kubo formula for transport coefficient:

$$\kappa = \frac{1}{k_B T^2 aN} \int_0^\infty \langle J(t)J(0)\rangle\, dt. \tag{113}$$

For the special case of heat conduction in one-dimensional chain, it is better to call κ heat conductance rather than heat conductivity. In analogous to electric circuit, the heat conductance relates the temperature gradient to energy current (Fourier law),

$$I = -\kappa \frac{dT}{dx}. \tag{114}$$

The quantity $J(t)$ is related to energy current by $J = IaN$.

The central quantity that we compute in equilibrium and nonequilibrium heat conduction is the (total) heat current J. Since the heat current is a macroscopic concept determined by the conservation of (internal) energy, a microscopic version of it is not unique. The current expression must satisfy the energy continuity equation in the long-wave limit. We derive an expression starting from $\mathbf{J} = \sum_i d(\mathbf{r}_i h_i)/dt$, where the local energy per particle is $h_i = \frac{1}{4}K_r\big((|\Delta\mathbf{r}_{i-1}| - a)^2 + (|\Delta\mathbf{r}_i| - a)^2\big) + K_\phi \cos\phi_i + p_i^2/(2m)$. By regrouping some of the terms using translational invariance, we arrive at the heat cur-

rent per particle:

$$
\begin{aligned}
m\mathbf{j}_i =\ & -\Delta\mathbf{r}_i\big((\mathbf{p}_i + \mathbf{p}_{i+1})\cdot\mathbf{G}(i)\big) \\
& -\Delta\mathbf{r}_{i-1}\big((\mathbf{p}_i + \mathbf{p}_{i-1})\cdot\mathbf{G}(i-1)\big) \\
& +\Delta\mathbf{r}_{i-1}\big(\mathbf{p}_i\cdot\mathbf{H}(i-2,i-1,i-1)\big) \\
& +\Delta\mathbf{r}_i\big(\mathbf{p}_i\cdot\mathbf{H}(i+1,i+1,i)\big) + \mathbf{p}_i h_i, \tag{115}
\end{aligned}
$$

where $\mathbf{G}(i) = \frac{1}{4}K_r\big(|\Delta\mathbf{r}_i| - a\big)\mathbf{n}_i$, $\mathbf{H}(i,j,k) = K_\phi(\mathbf{n}_i + \mathbf{n}_k \cos\phi_j)/|\Delta\mathbf{r}_k|$, $\mathbf{n}_i$ is a unit vector in direction of $\Delta\mathbf{r}_i = \mathbf{r}_{i+1} - \mathbf{r}_i$. The total heat current in x direction, $J = \sum_i j_{x,i}$ is the quantity appearing in the Green-Kubo formula. It is equal to the macroscopic heat current density (energy per unit area per unit time) integrated over a volume.

For theoretical analysis, we need to express J in terms of the dynamical variables P_k and Q_k. A general expression will be rather complicated. Again as in mode-coupling approach, we'll consider small oscillation expansions, and consider only the leading contributions. Neglecting the nonlinear contribution of $O(Q_k^3)$, we obtain

$$J = \sum_{k,\mu} b_k^\mu Q_k^\mu P_{-k}^\mu, \quad b_k^\mu = i\,\omega_k^\mu \frac{\partial \omega_k^\mu}{\partial\left(\frac{2\pi k}{Na}\right)}, \tag{116}$$

where ω_k^μ is the bare dispersion relation given by Eqs. (45) and (46). More general expression in a quantum-mechanical framework including the cubic terms is given in ref. [42].

An approximation for the correlation function of the current can be obtained, again using a dynamic mean-field approximation, as

$$
\begin{aligned}
\langle J(t)J(0)\rangle =\ & \sum_{k,\mu} |b_k^\mu|^2 \big\{ \langle Q_k^\mu(t)Q_{-k}^\mu(0)\rangle\langle P_k^\mu(t)P_{-k}^\mu(0)\rangle \\
& + \langle Q_k^\mu(t)P_{-k}^\mu(0)\rangle^2 \big\}. \tag{117}
\end{aligned}
$$

The above expression can be further simplified by the approximation $P_k^\mu = \dot{Q}_k^\mu \approx \tilde{\omega}_k^\mu Q_k^\mu$. We find

$$
\begin{aligned}
\langle J(t)J(0)\rangle &\approx \sum_{k,\mu} \left|\frac{b_k^\mu}{\beta\tilde{\omega}_k^\mu}\right|^2 g_k^\mu(t)^2 \\
&\approx \frac{aN(c^\parallel)^2}{2\pi\beta^2} \int_0^\infty \cos^2(\tilde{\omega}_p^\parallel t)\, e^{-2\gamma_p^\parallel t} dp \\
&\propto \frac{N(c^\parallel)^2}{\beta^2} t^{-1/(2-\delta_\parallel)}. \tag{118}
\end{aligned}
$$

We have dropped the contribution from the perpendicular component, because it decays much faster (due to an extra p^4 factor in the integrand).

We compare the mode-coupling result of Green-Kubo integrand with that of MD in Fig. 10. We have used Eq. (117) for the mode-coupling calculation. Note that the correlation functions $\langle Q(t)Q(0)^*\rangle$, $\langle P(t)P(0)^*\rangle$, and $\langle Q(t)P(0)^*\rangle$ are simply related in frequency domain through Eq. (32). The agreement is reasonable with the
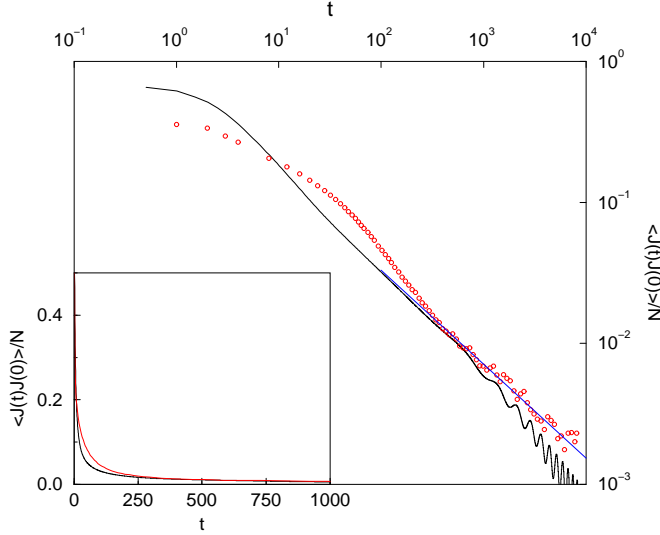
FIG. 10: The Green-Kubo integrand from MD (circles) and mode-coupling theory (curve) for set E with size $N = 1024$. The straight has a slope $-2/3$. The insert shows the same data on a linear scale.
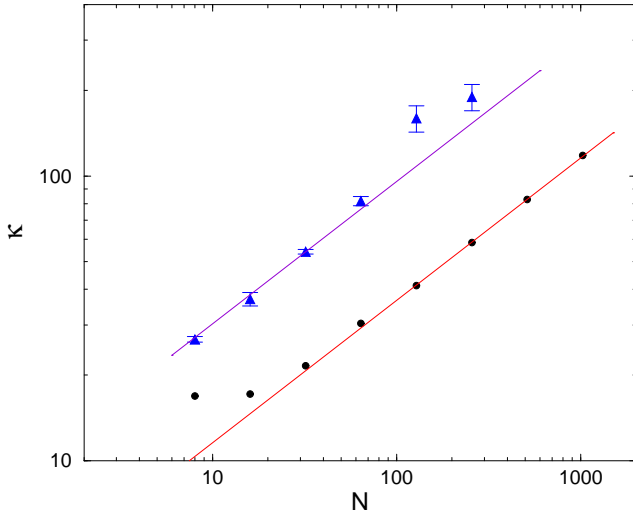

FIG. 11: The finite lattice conductance defined by Green-Kubo formula at parameter set E. Solid circles are from full mode-coupling theory; the triangles are from molecular dynamics with periodic boundary condition; the straight lines have slope of $1/2$.

largest deviation about a factor of 2. The asymptotic behavior of $t^{-2/3}$ is consistent with both sets of results.

The heat conductance on a finite lattice is sensitive to boundary conditions. Clearly, in the mode-coupling formulation, we have used periodic boundary condition. If we integrate over time from 0 to ∞ first on the second line of Eq. (118), we obtain $\kappa \propto \int dp/\gamma_p$. On a finite lattice we have a lower momentum cut-off, $2\pi/(Na)$. The size dependence of the conductance on finite lattice is

then

$$\kappa_N \propto N^{1-\delta_\parallel}. \tag{119}$$

Since $\delta_\parallel = 1/2$, $\kappa \propto \sqrt{N}$. This result is in agreement with that of Deutsch and Narayan for a model (the random collision model) where transverse motion is taken into account only stochastically [16].

In Fig. 11, the mode-coupling result of κ_N is compared with equilibrium molecular dynamics result with periodic boundary conditions. Excellent $1/2$ power is observed for the mode-coupling result. We found it is rather difficult to get converged value from molecular dynamics. But the results are consistent with a $\sqrt{N}$ law.

The relation of the mode-coupling theory with the results of nonequilibrium situation of low and high temperature heat-baths at the ends is not clear cut. The standard assumption is that the correlation should be cut off by a time scale of order N due to the interaction with the heat baths. Finite size result is obtained by integrating the power-law decay to a time of $O(N)$. This gives us the asymptotic behavior for the conductance at large N as

$$\kappa_N \propto N^\alpha, \quad \alpha = 1 - \frac{1}{2 - \delta_\parallel}. \tag{120}$$

Since we find $\delta_\parallel = 1/2$ for small $K^\perp$, the thermal conduction diverges as $N^{1/3}$. When $K^{(3)}$ is sufficiently large, we observe $N^{2/5}$.

VII. NONEQUILIBRIUM MOLECULAR DYNAMICS STUDY

A. MD simulation details

We note that the interaction potential is not smooth at the point when two particles overlap. This can cause numerical instability. Thus, we replaced the original potential with a modified one,

$$\Delta r = |\mathbf{r}_{i+1} - \mathbf{r}_i| \quad \rightarrow \quad \Delta r' = \Delta r + \frac{\epsilon^2}{\Delta r + \epsilon}, \tag{121}$$

which smooths out the discontinuous derivatives at $\Delta r = 0$ with a small correction of order ϵ^2. In addition to replacing the spring potential by $\frac{1}{2}K_r(\Delta r' - a)^2$, we also replace the cosine term by

$$\cos \phi_i' = -\frac{\Delta \mathbf{r}_{i-1} \cdot \Delta \mathbf{r}_i}{\Delta r_{i-1}' \Delta r_i'}, \tag{122}$$

so that the value is well-defined for all positions $\mathbf{r}_i$.

In actual simulation, we have used very small $\epsilon \sim 10^{-3}$ to 10^{-4} so that its effect should be comparable to error caused by finite time-step h. We also used large ϵ as a way of simulating a slightly different model to study the robustness of the results.

We solve the system of equations [41]

$$\frac{d\mathbf{p}_i}{dt} = \begin{cases} \mathbf{f}_i - \xi_L \mathbf{p}_i, & \text{if } i < N_w; \\ \mathbf{f}_i, & \text{if } N - N_w > i \geq N_w; \\ \mathbf{f}_i - \xi_H \mathbf{p}_i, & \text{if } i \geq N - N_w; \end{cases} \quad (123)$$

where $\mathbf{f}_i$ is the total force acting on the i-th particle, ξ_L and ξ_H obey the equation

$$\frac{d\xi_{L,H}}{dt} = \frac{1}{\Theta^2}\left(-1 + \frac{1}{k_B T_{L,H} N_w}\sum_i \frac{\mathbf{p}_i^2}{m}\right), \quad (124)$$

where T_L and T_H are the temperatures of the two heat baths at the ends. The summation is over the particles belonging to the heat bath. We have used 4 particles for the Nosé-Hoover heat baths, with extra first two and last two particles at fixed positions. The coupling parameter Θ is taking to be 1. For the central part, we used a second-order symplectic algorithm (or equivalently, the velocity Verlet algorithm), while for the heat-bath, we used a simple difference scheme accurate to second order in h for ξ.

Although the total energy (Hamiltonian) is no longer a conserved quantity when the heat-bath is introduced, the above equation still has a conserved quantity of similar character:

$$H(p,q) + \sum_{x=L,H} N_w k_B T_x \left(\frac{1}{2}\Theta^2\xi_x^2 + \int_0^t \xi_x dt\right). \quad (125)$$

This quantity can be used to monitor the stability of the algorithm.

Since we run for very long time steps of 10^8 to 10^{10}, it is essential that the algorithm is stable over extended period of time. Even with a symplectic algorithm, stability is not guaranteed by merely taking small h ($\sim 10^{-4}$). Thus, we adjusted the conserved quantity, Eq. (125), to its starting value after certain number of steps.

B. Heat conductance results

In Fig. 12, we observe that good temperature profiles are established. Due to relatively large temperature difference between low and high temperature heat baths, and perhaps also due to the nature of heat baths, the profile is not linear. However, the scaling with N is approximately obeyed.

In addition to the thermal conductance results reported in ref. [31], Fig. 13 gives additional data for variety of parameters. One of the aim of these additional runs is to check the robustness of the 1/3 power law for thermal conductance. It is found in ref [31] for set E exponent $\alpha = 0.334 \pm 0.003$. This is an excellent confirmation of the mode-coupling theory. We note that at parameter set K, the 1/3 law is not destroyed by introducing large ϵ. Thus we believe that the 1/3 law is not specific to the potential used in ref. [31]. In fact, the Fermi-Pasta-Ulam
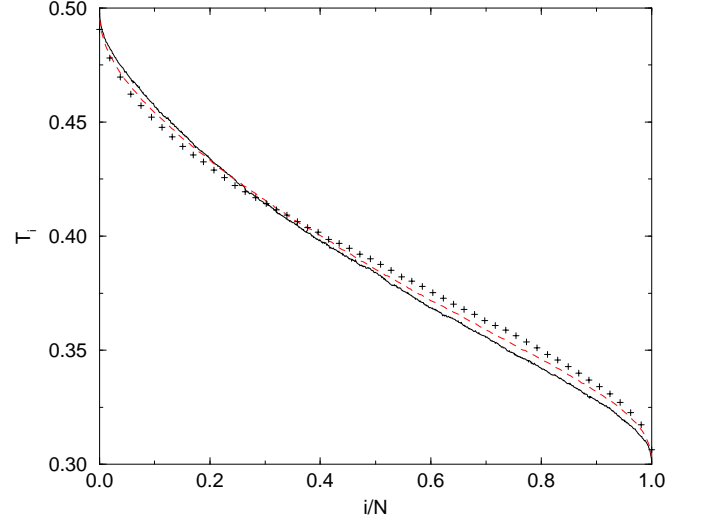

FIG. 12: Temperature of i-th particle, T_i vs scaled position, i/N, for data set E with $N = 64$ (plus), 256 (dash line), and 1024 (solid line).
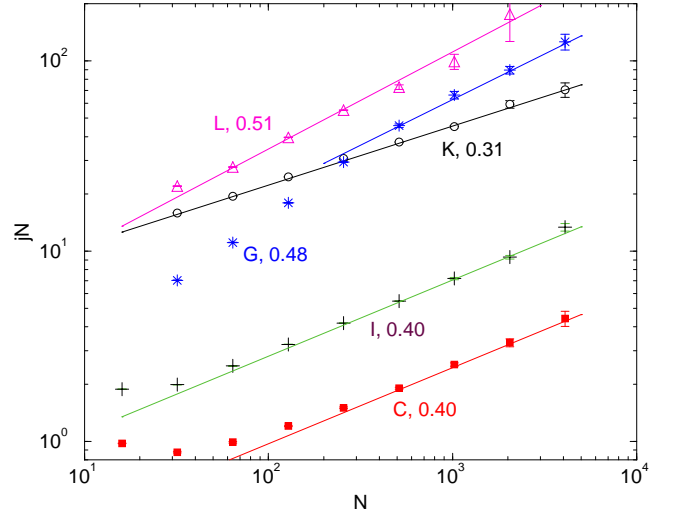

FIG. 13: jN vs N for different parameters $(K_\phi, T_L, T_H, \epsilon)$. set C: $(K_\phi, T_L, T_H, \epsilon) = (0.1, 0.2, 0.4, 0)$, the chain is compressed to have an average distance between particle $d_0 = 1.5$; set G: (10, 0.2, 0.4, 0); set I: (0.1, 0.3, 0.5, 0.2); set K: (0.5, 1.2, 2, 0.4); set L: (25, 1, 1.5, 0.2). All of the sets have $K_r = 1$, mass $m = 1$, and lattice constant $a = 2$. The number indicates the slope of least-squares fit.

model with transverse motion was studied [43] and result is also consistent with the 1/3 power law.

At low temperatures for set I and C, we appear to observe exponent of 0.4. What is particularly interesting for set C is that the chain is compressed to an average distance of 1.5 from the equilibrium distance of 2. The behavior is not changed much comparing to uncompressed chain. Set G and L represent very large angular

coupling K_ϕ. We note that $K_\phi \to \infty$ corresponds to a situation that equilibrium can not be established. As K_ϕ becomes larger, the equilibration becomes increasingly difficult. In ref. [31] we reported a logarithmic behavior for $K_\phi = 1$ (set B). This logarithmic behavior does not maintain when K_ϕ is increased further. The exponent α for set L and G is closed to $1/2$. This may be related the results of disordered harmonic chain.

VIII. CONCLUSION

Lepri *et al* first introduced mode-coupling theory into the problem of heat conduction in low dimensional systems to interpret the MD results qualitatively. We have developed the theory further by introducing a 'full theory' and effective parameters for theory. The full theory is solved numerically. At this level of approximation, we find that mode-coupling theory gives excellent prediction on a quantitative level. The longitudinal damping (decay rate) $\gamma_k^{\parallel}$ agrees with MD data with few per cents of deviation. The mode-coupling theory somewhat overestimated the transverse damping $\gamma_k^{\perp}$ by a factor of two to three. The full theory assumes that the damping function (memory kernel) $\Gamma_k[z]$ is an explicit function of two variables, k and z. In a simple mode-coupling theory, we assume $\Gamma_k[z] \approx (2\pi k/(Na))^2 \nu[z]$, valid for small k/N. The simple theory is computationally efficient, and contains essential asymptotic features, i.e., $\gamma_k^{\parallel} \propto k^{3/2}$ and $\gamma_k^{\perp} \propto k^2$. Through detailed comparison between MD and mode-coupling theory on memory kernel, decay of the modes, the time-dependent correlation functions, Green-Kubo integrand, and finally the finite-size conductance, we have strong evidence that the mode-coupling theory is correct, and it captures the essential features of the system.

We have used parameter set E as the main data set for comparison. The reason for choosing this particular set of parameters is that it gives the cleanest power-law behavior. Other parameters will be either qualitatively similar, or crossovers will be observed. In fact mode-coupling theory naturally predicts crossover, due to the presence of $K^{(3)}$ term. When this term is dominant, or the transverse effect can be neglected, we should see behavior of $\kappa \propto N^{2/5}$. Thus we feel that the controversy of the result of Lepri *et al* [6] and that of Narayan and Ramaswamy ($\kappa \propto N^{1/3}$) [15] can be reconciled within the current mode-coupling theory.

[1] R. E. Peierls, *Quantum Theory of Solids*, Chap. 2, (Oxford University Press, 1955).
[2] Z. Rieder, J. L. Lebowitz, and E. H. Lieb, J. Math. Phys. **8**, 1073 (1967).
[3] T. Prosen and D. K. Campbell, Phys. Rev. Lett. **84**, 2857 (2000).
[4] F. Bonetto, J. L. Lebowitz, L. Rey-Bellet, in *Mathematical Physics 2000*, p. 128, A. Fokas *et al.* (eds) (Imperial College Press, London, 2000).
[5] S. Lepri, R. Livi, and A. Politi, Phys. Rep. **377**, 1 (2003).
[6] S. Lepri, R. Livi, A. Politi, Europhys. Lett. **43**, 271 (1998).
[7] Y. Pomeau and P. Résibois, Phys. Rep. **19**, 63 (1975).
[8] U. Balucani and M. Zoppi, *Dynamics of the Liquid State*, (Oxford, 1994).
[9] S. Lepri, Phys. Rev. E **58**, 7165 (1998).
[10] A. Perverzev, Phys. Rev. E **68**, 056124 (2003).
[11] H. Kaburaki and M. Machida, Phys. Lett. A**181**, 85 (1993).
[12] S. Lepri, R. Livi, and A. Politi, Phys. Rev. Lett. **78**, 1896 (1997).
[13] S. Lepri, Eur. Phys. J. B **18**, 441 (2000).
[14] B. Hu, B. Li, and H. Zhao, Phys. Rev. E **61**, 3828 (2000).
[15] O. Narayan and S. Ramaswamy, Phys. Rev. Lett. **89**, 200601 (2002).
[16] J. M. Deutsch and O. Narayan, Phys. Rev. E **68**, 010201(R) (2003); Phys. Rev. E **68**, 041203 (2003).
[17] P. Grassberger, W. Nadler and L. Yang, Phys. Rev. Lett. **89**, 180601 (2002).
[18] A. Dhar, Phys. Rev. Lett., **86**, 3554 (2001); G. Casati and T. Prosen, Phys. Rev. E **67**, 015203 (R) (2003).
[19] S. Lepri, R. Livi, A. Politi, Phys. Rev. E **68**, 067102 (2003).
[20] B. Hu, B. Li and H. Zhao, Phys. Rev. E **57**, 2992 (1998).
[21] K. Aoki and D. Kusnezov, Phys. Lett. B **477**, 348 (2000).
[22] B. Li, L. Wang, and B. Hu, Phys. Rev. Lett. **88**, 223901 (2002); B. Li, G. Casati, and J. Wang, Phys. Rev. E **67**, 021204 (2003); B. Li, G. Casati, J. Wang, and T. Prosen, cond-mat/0307692; D. Alonso, R. Artuso, G. Casati, and I. Guarneri Phys. Rev. Lett. **82**, 1859 (1999); D. Alonso, A. Ruiz, and I. de. Vega, Phys. Rev. E **66**, 066131 (2002).
[23] B. Li and J. Wang, Phys. Rev. Lett. **91**, 044301 (2003); *ibid.*, **92**, 089402 (2004).
[24] M. Terraneo, M. Peyrard, and G. Casati, Phys. Rev. Lett **88**, 094302 (2002).
[25] S. Berber, Y.-K. Kwon, and D. Tománek, Phys. Rev. Lett. **84**, 4613 (2000).
[26] J. Che, T. Çağin, and W. A. Goddard III, Nanotechnology, **11**, 65 (2000).
[27] S. Maruyama, Physica B **323**, 193 (2002).
[28] Z. Yao, J.-S. Wang, B. Li, and G.-R. Liu, cond-mat/0402616; G. Zhang and B. Li, NUS-report (2004).
[29] Q. Zheng, G. Su, J. Wang, and H. Guo, Eur. Phys. J. B **25**, 233 (2002).
[30] T. Yamamoto, S. Watanabe, K. Watanabe, cond-mat/0312600.
[31] J.-S. Wang and B. Li, Phys. Rev. Lett. **92**, 074302 (2004).
[32] L. I. Manevitch and A. V. Savin, Phys. Rev. E **55**, 4713 (1997); A. V. Savin and L. I. Manevitch, *ibid.* **61**, 7065 (2000); A. V. Savin, L. I. Manevitch, P. L. Christiansen, and A. V. Zolotaryuk, Physics-Uspekhi **42**, 245 (1999).

[33] S. L. Mayo, B. D. Olafson, and W. A. Goddard III, J. Phys. Chem. **94**, 8897 (1990).

[34] J. Tersoff, Phys. Rev. B **38**, 6991 (1988).

[35] R. Kubo, M. Toda, and N. Hashitsume, *Statistical Physics II*, pp.97-108, 2nd ed. (Springer, Berlin, 1992).

[36] R. Zwanzig, J. Chem. Phys. **33**, 1338 (1960).

[37] H. Mori, Prog. Theor. Phys. **33**, 424 (1965).

[38] K. Huang, *Statistical Mechanics*, 2nd, John Wiley, 1987.

[39] J. Scheipers and W. Schirmacher, Z. Phys. B. **103**, 547 (1997).

[40] E. Buckingham, Phys. Rev. **4**, 345 (1914).

[41] For general aspects on molecular dynamics, see, e.g., D. Frenkel and B. Smit, *Understanding Molecular Simulation: from algorithms to applications*, (Academic Press, 1996).

[42] R. J. Hardy, Phys. Rev. **132**, 168 (1963).

[43] B. Li, J.-H. Lan, and L. Wang, unpublished.